

## LETTER

# Biological synthesis of $\text{Fe}_3\text{O}_4@\text{Ag}$ using *Scenedesmus obliquus* and evaluation of its effect on the expression of *MexA-B* efflux pump genes in ciprofloxacin-resistant *Pseudomonas aeruginosa* strains

Sara Hadad<sup>1</sup> | Tabarek Abdulrazaq Alkinani<sup>2</sup> | Aida Mahmoudi<sup>3</sup> | Somayeh Dehghan<sup>4</sup> |  
Nastaran Maleki Moaf<sup>5</sup> | Akram Sadat Naeemi<sup>6</sup> | Ali Salehzadeh<sup>1</sup>

<sup>1</sup>Department of Biology, Rasht Branch, Islamic Azad University, Rasht, Iran

<sup>2</sup>Department of Biology, Science and Research Branch, Islamic Azad University, Tehran, Iran

<sup>3</sup>Department of Biology, Damghan Branch, Islamic Azad University, Damghan, Iran

<sup>4</sup>Department of Biology, Central Tehran Branch, Islamic Azad University, Tehran, Iran

<sup>5</sup>Department of Biology, Lahijan Branch, Islamic Azad University, Lahijan, Iran

<sup>6</sup>Department of Biology, Faculty of Science, University of Guilan, Rasht, Iran

## Correspondence

Ali Salehzadeh, Department of Biology, Rasht Branch, Islamic Azad University, Rasht, Iran  
Email: salehzadeh@iaurasht.ac.ir

## Abstract

This study was conducted to biosynthesize  $\text{Fe}_3\text{O}_4@\text{Ag}$  nanocomposite with *Scenedesmus obliquus* extract, and to evaluate its antibacterial potential against *Pseudomonas aeruginosa*. In addition, the effect of the synthesized nanocomposite on the expression of *MexA-B* efflux pump genes was investigated. The  $\text{Fe}_3\text{O}_4@\text{Ag}$  nanocomposite was characterized using X-ray diffraction spectroscopy (EDX), Fourier transform infrared spectroscopy (FT-IR), transmission electron microscopy (TEM), Dynamic light scattering (DLS) as well as Zeta potential analyses. Minimum inhibitory concentration (MIC) of the nanocomposite alone and in combination with ciprofloxacin against *P. aeruginosa* strains was determined. Finally, the expression of *MexA-B* efflux pump genes among the bacteria treated with the nanocomposite was evaluated using quantitative real-time PCR. Based on the results, the proper synthesis of the nanocomposite with the diameter of 40 to 70 nm and acceptable stability was confirmed. The synthesized nanocomposite had lower MIC value (8–64  $\mu\text{g}/\text{mL}$ ) than ciprofloxacin (64–512  $\mu\text{g}/\text{mL}$ ) which shows stronger antibacterial potential of the nanocomposite. In addition, treating bacteria with the nanocomposite and ciprofloxacin caused a significant reduction of *MexA-B* genes compared to the cells treated with ciprofloxacin or nanocomposite alone. Thus,  $\text{Fe}_3\text{O}_4@\text{Ag}$  nanocomposite can improve the efficacy of ciprofloxacin against *P. aeruginosa* by reducing the expression of *MexA-B* efflux pump genes.

## KEYWORDS

Ciprofloxacin, Efflux pump, Nanocomposite, *Pseudomonas aeruginosa*

## 1 | INTRODUCTION

*Pseudomonas aeruginosa*, an opportunistic Gram-negative pathogen, is an important human pathogen that is involved with several infections in both nosocomial and community-acquired cases, especially in burns and patients suffering from cystic fibrosis [1–3]. This bacterium is known to be able to develop resistance to a variety of antibacterial agents, which is attributed to drug inactivation, impermeability of bacterial outer membrane and activity of bacterial efflux systems [4]. Active expulsion of antibacterial drugs mediated by efflux systems including, *MexAB-oprM*, *MexCD-oprY*, *MexEF-*

*oprN*, *MexXY-oprM*, and *mexJKoprM* is regarded as a major important mechanism for development of drug resistance in *P. aeruginosa* strains [4, 5]. Intrinsic resistance to fluoroquinolones including, ciprofloxacin, norfloxacin and levofloxacin in *P. aeruginosa* has been reported to be mainly associated with bacterial efflux system and *MexAB-oprM* plays an important role in this issue [6]. Previous reports showed that inhibition of *MexAB-oprM* efflux pump system can potentiate the activity of fluoroquinolones [4, 7].

In recent years, metal nanoparticles are being used as efficient antimicrobial agents. Efficiency of several nanoparticles, individually or in combination with antibiotics, against pathogenic

This is an open access article under the terms of the [Creative Commons Attribution-NonCommercial-NoDerivs](https://creativecommons.org/licenses/by-nc-nd/4.0/) License, which permits use and distribution in any medium, provided the original work is properly cited, the use is non-commercial and no modifications or adaptations are made.

© 2022 The Authors. *Micro & Nano Letters* published by John Wiley & Sons Ltd on behalf of The Institution of Engineering and Technology.

bacteria have been reported [1, 8]. In addition, several metal nanoparticles have displayed efflux pump inhibitory potential which can recover potency of antibiotics [9–12]. Due to strong antibacterial activity, silver-based nanoparticles are widely used in different applications [8, 13]. Conjugation of magnetic compounds to metal nanoparticle is a novel approach in nanotechnology. Among magnetic compounds, magnetite ( $\text{Fe}_3\text{O}_4$ ) nanoparticles have gained attention due to their high magnetism, small size, biocompatibility as well as low toxicity [11, 14, 15]. Thus, conjugation of metal nanoparticles to  $\text{Fe}_3\text{O}_4$ , as a magnetic vector, results in several advantages including, site-directed delivery, easier recovery, and recyclability [15].

The preparation of metal nanoparticles can be accomplished using physio-chemical or biological methods. Since physio-chemical methods are involved with high expense and several environmental concerns, in recent years, green synthesis of nanoparticles via clean, eco-friendly and non-toxic methods using living organisms has gained attention [16, 17]. Algal species have been extensively used for the biosynthesis of metal nanoparticles. Antibacterial properties of  $\text{Fe}_3\text{O}_4@Ag$  nanocomposite against pathogenic bacteria have been reported previously [15], however, their effect on bacterial efflux pumps at the molecular level has rarely been investigated. Thus, in the present work, we aimed for biogenic synthesis of  $\text{Fe}_3\text{O}_4@Ag$  nanocomposite using the extract from the microalga *Scenedesmus obliquus* and to investigate the effect of prepared nanocomposite on the expression of *MexA-B* efflux pump genes among ciprofloxacin-resistant *P. aeruginosa* strains.

## 2 | MATERIALS AND METHODS

### 2.1 | Bacterial strains

A total number of 70 *P. aeruginosa* strains were primarily isolated from clinical specimens including, blood, urine, wounds, sputum and burn exudates from the patients referring to the hospitals of Rasht, Gorgan, and Tehran (Iran). The bacteria were identified using conventional biochemical and molecular assays and antibiotic susceptibility profile of the strains was determined according to the CLSI guideline [18]. Then, ciprofloxacin-resistant strains were selected for further investigation.

### 2.2 | Preparation of $\text{Fe}_3\text{O}_4@Ag$ nanocomposite

$\text{Fe}_3\text{O}_4@Ag$  nanocomposite was synthesized using the extract from *S. obliquus*. In order to prepare the algal extract, 1.5 g of algal powder (Parsian microalgae Co, Rasht City, Iran) was added to 25 mL sterile distilled water, kept in a water bath of 55°C for 20 min and then, centrifuged at 6000 rpm for 10 min. The supernatant was filtered through a Whatman No.1 filter paper and stored at 4°C.

In order to synthesize  $\text{Fe}_3\text{O}_4@Ag$  nanocomposite, at first, 50 mg Iron oxide was added to 100 mL distilled water and sonicated for 30 min. Then, 20 mg  $\text{AgNO}_3$  was added to the solution and sonicated for a further 45 min. Then, 10 mL of algal extract was added to the mixture to reduce silver ions. The mixture was shaken for 24 h at 25°C and then, the synthesized nanocomposite was harvested using centrifugation at 12,000 rpm for 20 min and dried in a vacuum oven at 80°C for 8 h [18].

### 2.3 | Characterization of $\text{Fe}_3\text{O}_4@Ag$ nanocomposite

Characterization of the synthesized  $\text{Fe}_3\text{O}_4@Ag$  nanocomposite was performed using energy-dispersive X-ray (EDX) analysis (TESCAN MIRA3 FEG-SEM, Kohoutovice, Czech Republic), powder X-ray diffraction analysis (XRD) (X'Pert Pro, Malvern Panalytical, UK), Transmission electron microscopy (TEM) (Zeiss EM10C, Oberkochen, Germany) and Fourier-transform infrared spectrum (FTIR) (Spectrum Two Model, PerkinElmer, Waltham, USA) in the range of 500–4000  $\text{cm}^{-1}$  and a resolution of 1  $\text{cm}^{-1}$ . The average hydrodynamic size of synthesized nanocomposite was examined by Dynamic Light Scattering technique (DLS) and the physical stability of  $\text{Fe}_3\text{O}_4@Ag$  nanocomposite was determined using Zeta potential analyzer (Zetasizer Ver. 6.32, Malvern Panalytical, UK).

### 2.4 | Minimum inhibitory concentration

The minimum inhibitory concentration (MIC) value of  $\text{Fe}_3\text{O}_4@Ag$  nanocomposite and ciprofloxacin against *P. aeruginosa* strains was determined using the broth microdilution method according to the CLSI guideline [19]. In brief, different compounds were serially diluted (1:2) in 96 well polystyrene plates and thus, a gradient concentration of each compound was prepared (final concentration of 4–1024  $\mu\text{g/mL}$ ). The solvent of  $\text{Fe}_3\text{O}_4@Ag$  nanocomposite was DMSO and also DMSO was used as a negative control. The wells were inoculated with 100  $\mu\text{L}$  of fresh bacterial suspension with a cell population of  $1.5 \times 10^6$  CFU/mL. The plates were incubated at 37°C for 24 h and bacterial growth was monitored. The MIC was the lowest concentration of each compound which inhibited visible bacterial growth. The assay was performed in triplicates for each bacterial strain.

Finally, based on the MIC values, bacterial strains were grown in the media containing sub-inhibitory concentration (1/4 MIC) of either ciprofloxacin or  $\text{Fe}_3\text{O}_4@Ag$  nanocomposite as well as the media containing both agents (1/4 MIC of each agent). Incubation was performed for 18 h at 37°C and then, the cells were harvested using centrifugation (3500 rpm, 10 min) and subjected to molecular analysis. The cells grown in the medium without ciprofloxacin or nanocomposite were considered as control.

**TABLE 1** The sequence of the primers used in this study

Gene	Sequence (5'-3')	Tm(°C)	Product (bp)	Reference
<i>MexA</i> -forward	ACCTACGAGGCCGACTACCAG	63.3	252	[32]
<i>MexA</i> -reverse	GTTGGTCACCAGGGCGCCTTC	65.1		
<i>MexB</i> -forward	GTGTTTCGGCTCGCAGTACTC	60.1	244	[32]
<i>MexB</i> -reverse	AACCGTCGGGATTGACCTTG	59.4		
<i>rpsL</i> -forward	CGGCACTGCGTAAGGTATGC	60.8	314	[33]
<i>rpsL</i> -reverse	CCCGAAGGTCTTTACAC	56.5		

## 2.5 | Expression of *MexA-B* genes

In order to investigate the effect of  $\text{Fe}_3\text{O}_4@\text{Ag}$  nanocomposite on the expression of *MexA-B* efflux pump genes, bacterial total RNA was extracted using AccuZol bacterial total RNA extraction solution (Bioneer, South Korea) according to the manufacturer's protocol. Then, extracted RNA was subjected to DNase I (Fermentas, Germany) treatment to remove genomic DNA contamination. The quality and quantity of extracted RNA were evaluated using a nanodrop spectrophotometer and agarose gel electrophoresis.

Synthesis of cDNA was performed using a cDNA synthesis kit (Sinaclon., Iran) according to the manufacturer's guideline. Quantitative real-time polymerase chain reaction (qRT-PCR) was used to investigate the effect of  $\text{Fe}_3\text{O}_4@\text{Ag}$  nanocomposite on the expression of *MexA-B* efflux pump genes in *P. aeruginosa* strains. qRT-PCR was performed in triplicates using gene-specific primers (Table 1). The assay was performed in a final volume of 12.5  $\mu\text{L}$  containing 6.25  $\mu\text{L}$  SYBR Green master mix (Sinaclon., Iran), 0.5  $\mu\text{L}$  of forward and reverse primers, 0.5  $\mu\text{L}$  of the synthesized cDNA and 4.75  $\mu\text{L}$  of DEPC treated distilled water. The *rpsL* gene was selected as the internal reference gene and the relative expression of *MexA-B* genes was determined using the  $2^{-\Delta\Delta\text{CT}}$  method, as described previously [20].

## 2.6 | Statistical analysis

Statistical analyses were performed using the SPSS. 16.0 software. One-way analysis of variance (ANOVA) along with Post hoc analysis according to Tukey's Test method was used to uncover specific differences between group means, when ANOVA test was significant. The assays were performed in triplicates and *p*-values less than 0.05 were considered statistically significant.

## 3 | RESULTS

### 3.1 | Antibiotic susceptibility

Antibiotic susceptibility of *P. aeruginosa* strains was determined using the disk diffusion method. Based on the results, the highest resistance was observed toward gentamicin (47%),

**TABLE 2** Results of EDS analysis of nanocomposite

Elements	K	Kr	Weight %	Atomic %	ZAF
C	0.1604	0.1025	26.65	53.52	0.3844
O	0.0746	0.0476	16.65	25.10	0.2862
P	0.0188	0.0120	1.50	1.17	0.7997
Fe	0.5232	0.3342	37.79	16.32	0.8841
Ag	0.2230	0.1424	17.40	3.89	0.8185
Total	1.0000	0.6387	100.00	100.00	

followed by ciprofloxacin and imipenem (36%), while, amikacin and piperacillin were considered as the most efficient antibiotics with susceptibility of 83%. Susceptibility of *P. aeruginosa* strains to different antibiotics was presented in Figure 1.

### 3.2 | Characterization of $\text{Fe}_3\text{O}_4@\text{Ag}$ nanocomposite

Figure 2 shows the typical XRD pattern of the synthesized nanocomposite in a range of  $2\theta = 10-70^\circ$ . Eight characteristic sharp peaks (at  $2\theta = 17.89^\circ, 27.74^\circ, 32.13^\circ, 34.77^\circ, 46.17^\circ, 54.80^\circ, 57.35^\circ$ , and  $63.75^\circ$ ) are observed which are corresponding to (111), (220), (311), (222), (400), (422), (511), and (440) Bragg's reflections, respectively. The diffraction peaks can be indexed to the face-centred cubic structure of  $\text{Fe}_3\text{O}_4$ . In addition, the peaks at  $2\theta = 38.02^\circ, 43.66^\circ$ , and  $64.62^\circ$  correspond to the (111), (200), and (220) Bragg's reflections of Ag (JCPDS card no.04-0783). The results are similar to those reported previously [18].

The transmission electron microscopy image of  $\text{Fe}_3\text{O}_4@\text{Ag}$  nanocomposite was displayed in Figure 3. The image shows that the obtained particles are spherical and have diameters of 50–75 nm.

Elemental composition and distribution on the surface of the  $\text{Fe}_3\text{O}_4@\text{Ag}$  nanocomposite were surveyed using Energy-dispersive X-ray (EDX) analysis. The results clearly confirmed the presence of Fe, O and Ag in the synthesized nanocomposite (Figure 4 and Table 2).

The FT-IR spectra of the Ag NP,  $\text{Fe}_3\text{O}_4$  NP and biosynthesized  $\text{Fe}_3\text{O}_4@\text{Ag}$  nanocomposite are presented in Figures 5a, 5b and 5c respectively. The spectrum of biosynthesized  $\text{Fe}_3\text{O}_4@\text{Ag}$  nanocomposite showed the presence of

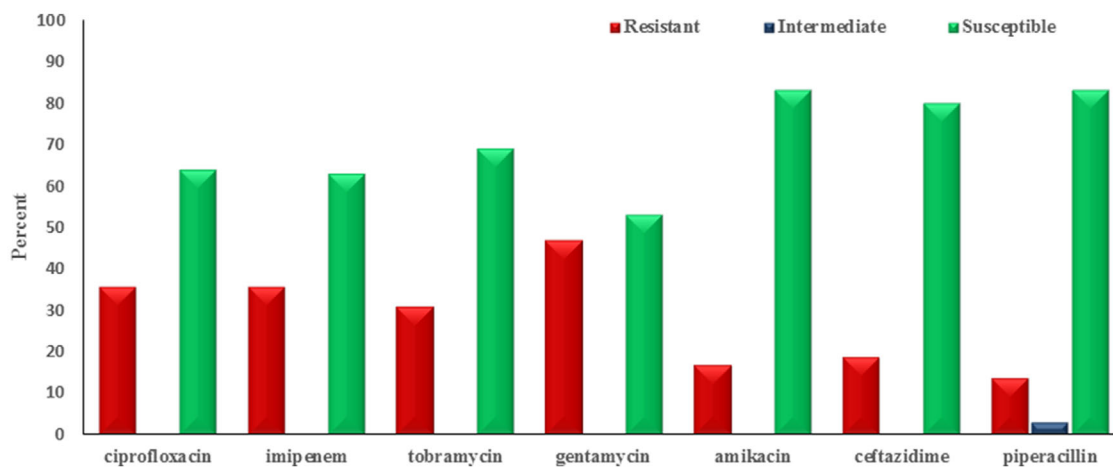


FIGURE 1 Antibiotic susceptibility of *P. aeruginosa* strains

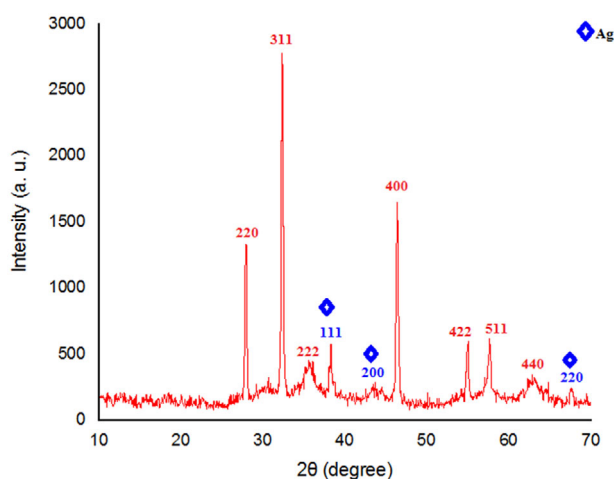


FIGURE 2 XRD pattern of  $\text{Fe}_3\text{O}_4@\text{Ag}$  nanocomposite

amino, carboxylic, hydroxyl, and carbonyl groups at the surface of nanocomposite. A broad band was observed around  $3415\text{ cm}^{-1}$ , which is associated with the overlapping of the stretching vibration of the primary and aromatic amine groups of algal extracted molecules and O–H stretching of water molecules adsorbed to the surface of nanoparticles [18].

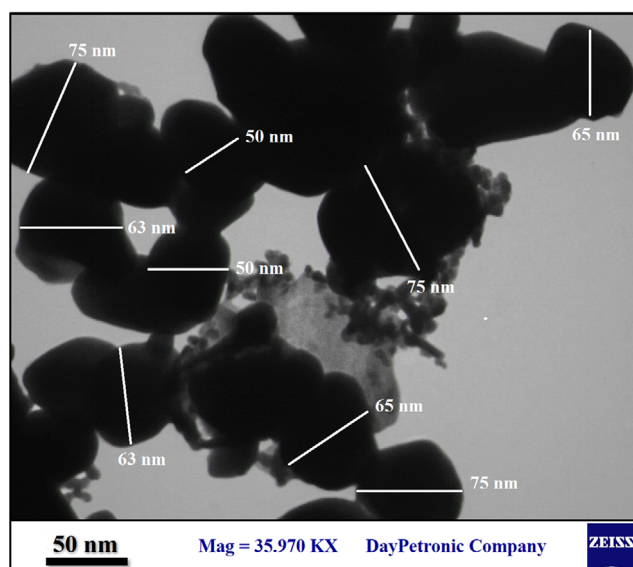


FIGURE 3 TEM image of synthesized  $\text{Fe}_3\text{O}_4@\text{Ag}$  nanocomposite. The size of particles is between 50 and 75 nm with spherical morphology

Absorption peaks around  $1637\text{ cm}^{-1}$  can be corresponding to the stretching vibrations of  $\text{C}=\text{O}$  moieties in carbonyl groups

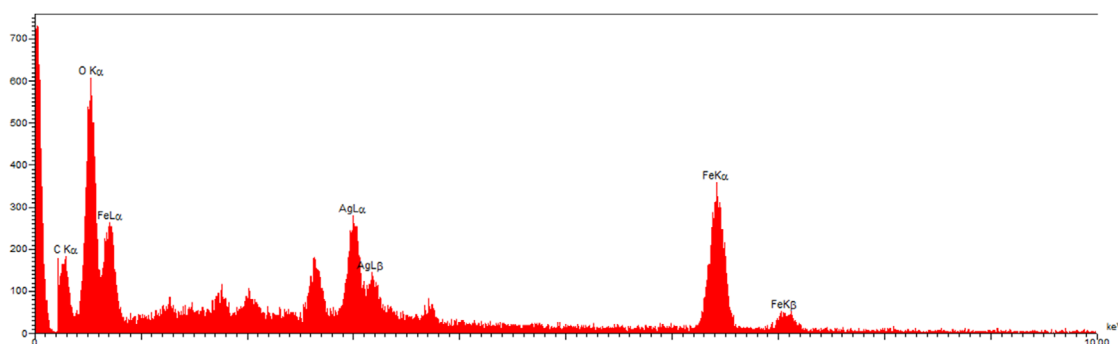
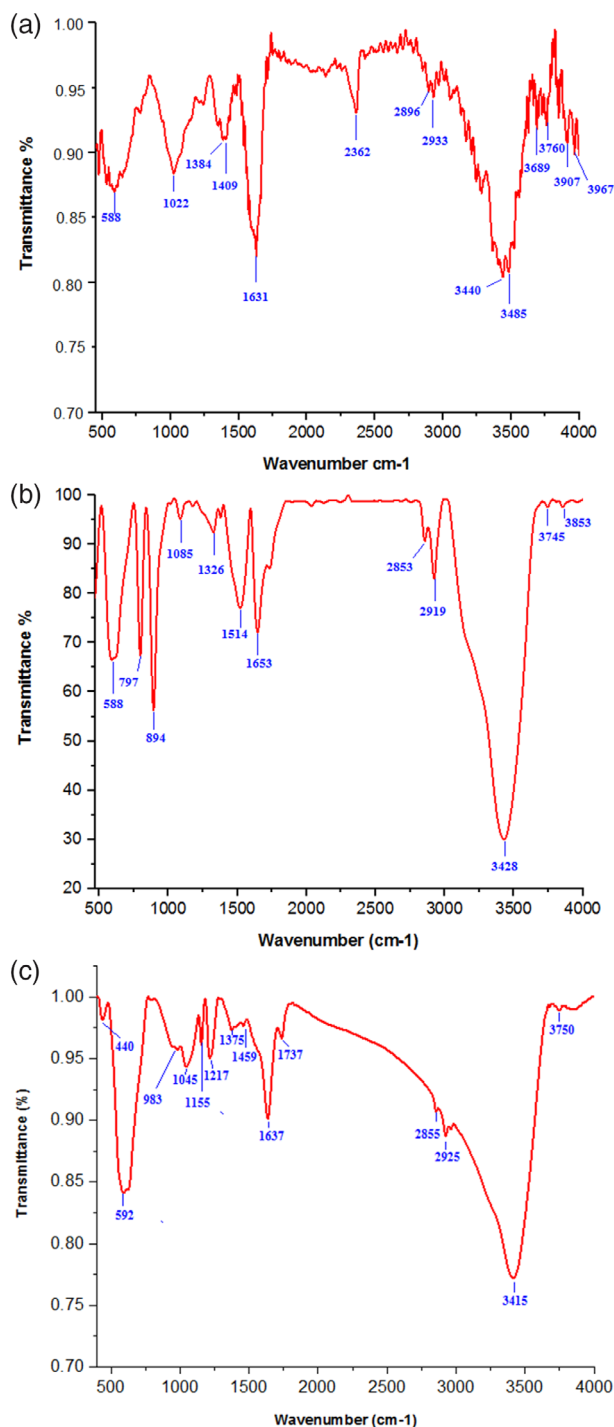


FIGURE 4 EDX image of the synthesized  $\text{Fe}_3\text{O}_4@\text{Ag}$  nanocomposite





**FIGURE 5** FT-IR spectra of the synthesized  $\text{Fe}_3\text{O}_4@\text{Ag}$  nanocomposite. (a) Ag NP, (b)  $\text{Fe}_3\text{O}_4$  NP and (c)  $\text{Fe}_3\text{O}_4@\text{Ag}$  nanocomposite

and aromatic  $\text{C}=\text{C}$  bond or intramolecular hydrogen bonds [21]. The band around  $1375\text{ cm}^{-1}$  is assigned to the  $\text{C}-\text{N}$  stretching vibration of aromatic amine or amid groups on the surface of  $\text{Fe}_3\text{O}_4@\text{Ag}$  nanoparticles which was not present in Ag NP and  $\text{Fe}_3\text{O}_4$  NP spectra. The peaks appeared at  $1217$  and  $1155\text{ cm}^{-1}$  can be attributed to the deformation of  $\text{C}-\text{O}-\text{H}$ ,  $\text{C}-\text{H}$  stretching of epoxy groups, and  $\text{C}-\text{O}$  alkoxy groups stretching, respectively [22]. The stretching frequency of

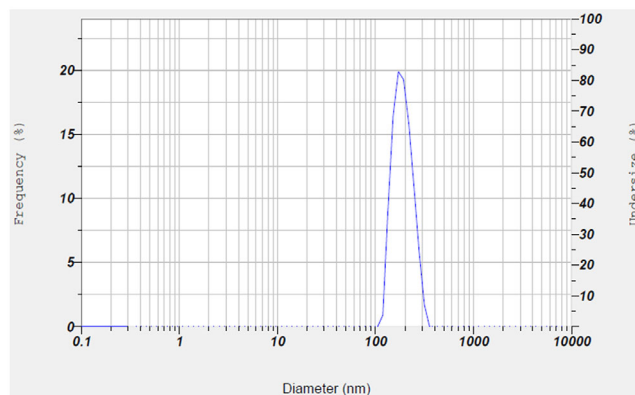


**FIGURE 6** Dynamic light scattering analysis of  $\text{Fe}_3\text{O}_4@\text{Ag}$  nanocomposite

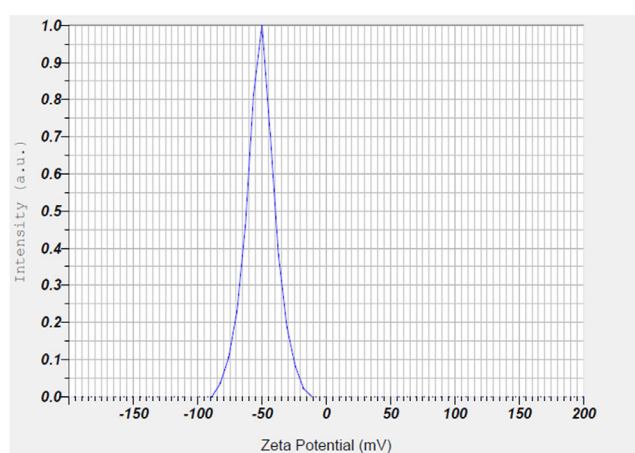


**FIGURE 7** Zeta potential analysis of  $\text{Fe}_3\text{O}_4@\text{Ag}$  nanocomposite

Metal—O in Ag NP and  $\text{Fe}_3\text{O}_4$  NP spectra is attributed to the band at  $588\text{ cm}^{-1}$ . The stretching frequency of Metal—O in final biosynthesized product ( $\text{Fe}_3\text{O}_4@\text{Ag}$  nanocomposite) is shifted to the bands at about  $592$  and  $440\text{ cm}^{-1}$ . Based on the FT-IR spectra of Ag NP,  $\text{Fe}_3\text{O}_4$  NP and biosynthesized  $\text{Fe}_3\text{O}_4@\text{Ag}$  nanocomposite, proper modification of the nanoparticles with the organic parts can be confirmed.

Dynamic light scattering is employed to analysis the hydrodynamic size of the magnetic nanoparticles. Figure 6 indicated the average particle size of  $\text{Fe}_3\text{O}_4@\text{Ag}$  nanocomposite was  $205\text{ nm}$ .

The stability of the particles was proved to be good as the zeta potential existed in the  $-50.9\text{ mV}$  range (Figure 7).

### 3.3 | MIC value

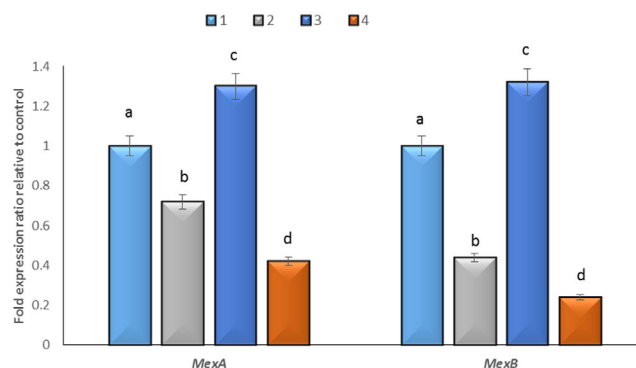
MIC value for  $\text{Fe}_3\text{O}_4@\text{Ag}$  nanocomposite and ciprofloxacin against *P. aeruginosa* strains was determined using the broth microdilution method. According to the results, MIC values of the synthesized nanocomposite were in a range of  $8\text{--}64\text{ }\mu\text{g/mL}$  while the MIC values for ciprofloxacin against bacterial strains were determined in a range of  $64\text{--}512\text{ }\mu\text{g/mL}$  (Table 3).

**TABLE 3** The MIC value of strains treated with Ciprofloxacin and Fe<sub>3</sub>O<sub>4</sub>@Ag

Number of bacterial strains	Treatment with Ciprofloxacin	Treatment with Fe <sub>3</sub> O <sub>4</sub> @Ag
1	64	16
2	128	16
3	256	32
4	128	64
5	128	32
6	512	32
7	256	16
8	64	8
9	512	16
10	128	8
11	64	16
12	128	16
13	512	8
14	128	64
15	128	32
16	256	8
17	128	32
18	128	16
19	256	16
20	256	8
21	512	16
22	64	64
23	256	16
24	128	32
25	256	16

### 3.4 | Expression of *MexA-B* genes

Quantitative RT-PCR was used for evaluation of the expression of *MexA-B* efflux pump genes among *P. aeruginosa* strains treated with ciprofloxacin and Fe<sub>3</sub>O<sub>4</sub>@Ag nanocomposite alone or in combination. Our results showed that treating *P. aeruginosa* with ciprofloxacin alone, cause overexpression of both efflux pump genes by 1.30- and 1.32-folds (compared with control cells) for *MexA* and *MexB* genes, respectively. Furthermore, treating bacteria with Fe<sub>3</sub>O<sub>4</sub>@Ag nanocomposite alone reduced the expression of both *MexA* and *MexB* genes by 0.28- and 0.56-folds, respectively, which was significantly stronger reduction than control cells (Figure 8). The highest reduction of efflux pump genes was observed among the cells simultaneously treated with both agents. In other words, the expression of *MexA* and *MexB* genes was reduced by 0.58- and 0.76-folds respectively, which was the strongest reduction of efflux pump genes compared with other treatments. Figure 6 displays the relative expression level of *MexA-B* efflux pump genes among *P. aeruginosa* strains treated with different compounds.

**FIGURE 8** Expression of *MexA-B* efflux pump genes among *P. aeruginosa* strains treated with different compounds. (a) Control; (b) Fe<sub>3</sub>O<sub>4</sub>@Ag nanocomposite; (c) ciprofloxacin; (d) Fe<sub>3</sub>O<sub>4</sub>@Ag nanocomposite + ciprofloxacin. Different letters mean significantly different

## 4 | DISCUSSION

*P. aeruginosa* is regarded as an important human pathogen, responsible for a variety of infections from simple infections to life-threatening ones [23]. This bacterium is well known for the intrinsic drug resistance potential. Although several mechanisms could be involved with the development of drug resistance in *P. aeruginosa* strains, the impermeability of bacterial outer membrane and drug expulsion by efflux pumps are regarded as two important mechanisms for the development of drug resistance [24]. Fluoroquinolones including, ciprofloxacin, are a class of antibiotics that prevent bacterial growth by inhibiting bacterial topoisomerase enzymes [25]. Ciprofloxacin is a commonly prescribed drug against a variety of bacterial infections. However, the development of ciprofloxacin resistance among *P. aeruginosa* strains has been increasing recently. According to our study, 36% of the isolated *P. aeruginosa* strains were resistant to ciprofloxacin, which is a remarkably high prevalence. The result was in accordance with previous research on the prevalence of ciprofloxacin resistance *P. aeruginosa* in the north of Iran, which showed a frequency of 39% [26].

In this study, we synthesized Fe<sub>3</sub>O<sub>4</sub>@Ag nanocomposite using the extract from the microalga, *S. obliquus*. Biosynthesis of metal nanoparticle using biological methods has several advantages compared to the physio-chemical methods including, lower expense and, avoiding harsh conditions and toxic chemicals. Biosynthesis of Fe<sub>3</sub>O<sub>4</sub>@Ag nanocomposite using algal and plant extracts has been reported, while, to our knowledge biosynthesis of Fe<sub>3</sub>O<sub>4</sub>@Ag nanocomposite using *S. obliquus* has not been studied. Characterization of the synthesized nanocomposite using TEM, XRD, EDX, FT-IR, DLS and Zeta potential analysis indicated proper synthesis of the particles and thus, biosynthesis using *S. obliquus* extract can be regarded as a good approach for the biosynthesis of Fe<sub>3</sub>O<sub>4</sub>@Ag nanocomposite.

The particle size measured by DLS was generally higher than the size of Fe<sub>3</sub>O<sub>4</sub>@Ag nanocomposite observed using TEM imaging. This difference in size, was due to the hydration layer surrounding the nanocomposite during the preparation of

$\text{Fe}_3\text{O}_4@\text{Ag}$  nanocomposite for DLS analysis. The zeta potential value for this nanocomposite was  $-50.9$  mV. The zeta potential value lower than  $-30$  and higher than  $+30$  indicates that the particles disperse well in media and the electrostatic repulsive force among the particles is large, and thus, the particles have good physical stability [27].

Bacterial inhibitory potential of  $\text{Fe}_3\text{O}_4@\text{Ag}$  nanocomposite against *P. aeruginosa* strains was evaluated. Based on the results, of  $\text{Fe}_3\text{O}_4@\text{Ag}$  nanocomposite had stronger bacterial inhibitory potential compared to the ciprofloxacin, which resulted in the lower MIC value. Several studies reported that Ag-based nanoparticles can inhibit bacterial cells via different mechanisms including, cell wall destruction, disruption of membrane selective permeability, prevention of DNA unwinding as well as direct inhibition of bacterial proteins [28–31]. Thus, it seems that the antibacterial potential of the synthesized composite is mainly attributed to the silver particles. It is noteworthy that, incorporation of  $\text{Fe}_3\text{O}_4$  into the nanocomposite provides magnetic properties that can be used for site-directed delivery and recyclability of the nanocomposite.

Expression of *MexA-B* efflux pump genes among *P. aeruginosa* strains treated with nanocomposite or ciprofloxacin alone, and in combination was investigated using qRT-PCR. Our results showed that, treating bacteria with ciprofloxacin induced expression of both the *MexA-B* efflux pump gene. *MexA-B* are involved with expulsion of fluoroquinolones and thus, overexpression of them in the presence of ciprofloxacin is predictable. Although, treating bacteria with nanocomposite alone and in combination with ciprofloxacin reduced the expression of both efflux pump genes, simultaneous treating of bacteria with both agents showed significantly higher efficacy in the reduction of *MexA-B*. As described above, Ag-based nanoparticles disrupt bacterial permeability by damaging cell wall and bacterial membranes. Inside the cell, metal nanoparticles can inhibit the enzymes responsible for normal cellular functions, and thus interfere with cellular functions including, DNA replication, transcription and translation. In addition, *P. aeruginosa* is well known for the impermeability of bacterial outer membrane to different antibacterial agents. Thus, a combination of  $\text{Fe}_3\text{O}_4@\text{Ag}$  nanocomposite with ciprofloxacin caused increased permeability of bacterial envelopes and thus, easier penetration of the drug into the cytoplasm. Inside the bacterial cells, the nanoparticles are able to inhibit bacterial enzymes via direct interaction with functional groups of proteins, which cause perturbation of cellular functions involved with gene expression. Furthermore, ciprofloxacin, as a member of fluoroquinolone drugs, is able to inhibit bacterial topoisomerases and thus, inhibit natural cellular functions involved with DNA unwinding [25]. Therefore, the synergistic effect of  $\text{Fe}_3\text{O}_4@\text{Ag}$  nanocomposite and ciprofloxacin in the reduction of *MexA-B* may be associated with non-specific inhibition of gene transcription.

## 5 | CONCLUSION

In the current work,  $\text{Fe}_3\text{O}_4@\text{Ag}$  nanocomposite was synthesized from *S. obliquus* extract and efficacy of the synthesized

nanocomposite in the reduction of *MeXA-B* efflux pump genes in ciprofloxacin-resistant *P. aeruginosa* strains was displayed. This research showed that  $\text{Fe}_3\text{O}_4@\text{Ag}$  nanocomposite could be considered as a candidate for combination therapy to potentiate the efficacy of ciprofloxacin against drug-resistant *P. aeruginosa*. However, further characterization of  $\text{Fe}_3\text{O}_4@\text{Ag}$  nanocomposite to be used in biomedical purposes is still required.

## FUNDING INFORMATION

The author(s) received no specific funding for this work

## CONFLICT OF INTEREST

The authors declare that they have no conflict of interest.

## DATA AVAILABILITY STATEMENT

The datasets generated during the current study are available from the corresponding author on reasonable request.

## REFERENCES

1. Abdolhosseini, M.; Zamani, H.; Salehzadeh, A.: Synergistic antimicrobial potential of ciprofloxacin with silver nanoparticles conjugated to thiosemicarbazide against ciprofloxacin resistant *Pseudomonas aeruginosa* by attenuation of *MexA-B* efflux pump genes. *Biologia* 74(9), 1191–1196 (2019)
2. Perez, L.; Antunes, A.; Freitas, A.; Barth, A.: When the resistance gets clingy: *Pseudomonas aeruginosa* harboring metallo- $\beta$ -lactamase gene shows high ability to produce biofilm. *Eur. J. Clin. Microbiol. Infect. Dis.* 31(5), 711–714 (2012)
3. Rasamiravaka, T.; El Jaziri, M.: Quorum-sensing mechanisms and bacterial response to antibiotics in *P. aeruginosa*. *Curr. Microbiol.* 73(5), 747–753 (2016)
4. Nakayama, K.; Ishida, Y.; Ohtsuka, M.; Kawato, H.; Yoshida, K.-i.; Yokomizo, Y.; Hosono, S.; Ohta, T.; Hoshino, K.; Ishida, H.: *MexAB-OprM*-specific efflux pump inhibitors in *Pseudomonas aeruginosa*. Part 1: Discovery and early strategies for lead optimization. *Bioorg. Med. Chem. Lett.* 13(23), 4201–4204 (2003)
5. Salehi, M.; Hekmatdoost, M.; Hosseini, F.: Quinolone resistance associated with efflux pumps *mexAB-oprM* in clinical isolates of *Pseudomonas aeruginosa*. *J. Microbial World.* 6(4), 290–298 (2014)
6. Renau, T.E.; Léger, R.; Flamme, E.M.; Sangalang, J.; She, M.W.; Yen, R.; Gannon, C.L.; Griffith, D.; Chamberland, S.; Lomovskaya, O.: Inhibitors of efflux pumps in *Pseudomonas aeruginosa* potentiate the activity of the fluoroquinolone antibacterial levofloxacin. *J. Med. Chem.* 42(24), 4928–4931 (1999)
7. Kriengkauykit, J.; Porter, E.; Lomovskaya, O.; Wong-Beringer, A.: Use of an efflux pump inhibitor to determine the prevalence of efflux pump-mediated fluoroquinolone resistance and multidrug resistance in *Pseudomonas aeruginosa*. *Antimicrob. Agents Chemother.* 49(2), 565–570 (2005)
8. Ahmed, K.B.A.; Raman, T.; Veerappan, A.: Future prospects of antibacterial metal nanoparticles as enzyme inhibitor. *Mater. Sci. Eng., C* 68, 939–947 (2016)
9. Christena, L.R.; Mangalagowri, V.; Pradheeba, P.; Ahmed, K.B.A.; Shalini, B.I.S.; Vidyalakshmi, M.; Anbazhagan, V.: Copper nanoparticles as an efflux pump inhibitor to tackle drug resistant bacteria. *RSC Adv.* 5(17), 12899–12909 (2015)
10. Nejabatdoust, A.; Salehzadeh, A.; Zamani, H.; Moradi-Shoeili, Z.: Synthesis, characterization and functionalization of ZnO nanoparticles by glutamic acid (Glu) and conjugation of ZnO@Glu by thiosemicarbazide and its synergistic activity with ciprofloxacin against multi-drug resistant *Staphylococcus aureus*. *J. Cluster Sci.* 30(2), 329–336 (2019)

11. Kahzad, N.; Salehzadeh, A.: Green synthesis of CuFe<sub>2</sub>O<sub>4</sub>@Ag nanocomposite using the *Chlorella vulgaris* and evaluation of its effect on the expression of *norA* efflux pump gene among *Staphylococcus aureus* strains. *Biol. Trace Elem. Res.* 198(1), 359–370 (2020)
12. Nejabatdoust, A.; Zamani, H.; Salehzadeh, A.: Functionalization of ZnO nanoparticles by glutamic acid and conjugation with thiosemicarbazide alters expression of efflux pump genes in multiple drug-resistant *Staphylococcus aureus* strains. *Microb. Drug Resist.* 25(7), 966–974 (2019)
13. Lin, L.; Cui, H.; Zeng, G.; Chen, M.; Zhang, H.; Xu, M.; Shen, X.; Bortolini, C.; Dong, M.: Ag–CuFe<sub>2</sub>O<sub>4</sub> magnetic hollow fibers for recyclable antibacterial materials. *J. Mater. Chem. B* 1(21), 2719–2723 (2013)
14. Salehzadeh, A.; Naeemi, A.S.; Khaknezhad, L.; Moradi-Shoeili, Z.; Shandiz, S.A.S.: Fe<sub>3</sub>O<sub>4</sub>/Ag nanocomposite biosynthesized using *Spirulina platensis* extract and its enhanced anticancer efficiency. *IET Nanobiotechnol.* 13(7), 766–770 (2019)
15. Venkateswarlu, S.; Kumar, B.N.; Prathima, B.; Anitha, K.; Jyothi, N.: A novel green synthesis of Fe<sub>3</sub>O<sub>4</sub>-Ag core shell recyclable nanoparticles using *Vitis vinifera* stem extract and its enhanced antibacterial performance. *Phys. B* 457, 30–35 (2015)
16. Sinha, S.N.; Paul, D.; Halder, N.; Sengupta, D.; Patra, S.K.: Green synthesis of silver nanoparticles using fresh water green alga *Pithophora oedogonia* (Mont.) Wittrock and evaluation of their antibacterial activity. *Appl. Nanosci.* 5(6), 703–709 (2015)
17. Narayanan, K.B.; Sakthivel, N.: Green synthesis of biogenic metal nanoparticles by terrestrial and aquatic phototrophic and heterotrophic eukaryotes and biocompatible agents. *Adv. Colloid Interface Sci.* 169(2), 59–79 (2011)
18. Shokoofeh, N.; Moradi-Shoeili, Z.; Naeemi, A.S.; Jalali, A.; Hedayati, M.; Salehzadeh, A.: Biosynthesis of Fe<sub>3</sub>O<sub>4</sub>@Ag nanocomposite and evaluation of its performance on expression of *norA* and *norB* efflux pump genes in ciprofloxacin-resistant *Staphylococcus aureus*. *Biol. Trace Elem. Res.* 191(2), 522–530 (2019)
19. CLSI, M100-S27: Performance standards for antimicrobial susceptibility testing; 27th informational supplement. (2017)
20. Pfaffl, M.W.: A new mathematical model for relative quantification in real-time RT–PCR. *Nucleic Acids Res.* 29(9), e45–e45 (2001)
21. Chandraker, K.; Nagwanshi, R.; Jadhav, S.; Ghosh, K.K.; Satnami, M.L.: Antibacterial properties of amino acid functionalized silver nanoparticles decorated on graphene oxide sheets. *Spectrochim. Acta, Part A* 181, 47–54 (2017)
22. Jain, N.; Bhargava, A.; Majumdar, S.; Tarafdar, J.; Panwar, J.: Extracellular biosynthesis and characterization of silver nanoparticles using *Aspergillus flavus* NJP08: A mechanism perspective. *Nanoscale* 3(2), 635–641 (2011)
23. Ding, Y.; Onodera, Y.; Lee, J.C.; Hooper, D.C.: NorB, an efflux pump in *Staphylococcus aureus* strain MW2, contributes to bacterial fitness in abscesses. *J. Bacteriol.* 190(21), 7123–7129 (2008)
24. Hancock, R.E.; Speert, D.P.: Antibiotic resistance in *Pseudomonas aeruginosa*: Mechanisms and impact on treatment. *Drug Resist. Updates* 3(4), 247–255 (2000)
25. Hooper, D.C.: Emerging mechanisms of fluoroquinolone resistance. *Emerging Infect. Dis.* 7(2), 337 (2001)
26. Shahandashti, E.F.; Molana, Z.; Asgharpour, F.; Mojtahedi, A.; Rajabnia, R.: Molecular detection of integron genes and pattern of antibiotic resistance in *Pseudomonas aeruginosa* strains isolated from intensive care unit, Shahid Beheshti Hospital, North of Iran. *Int. J. Mol. Cell. Med.* 1(4), 209 (2012)
27. Joseph, E.; Singhvi, G.: Multifunctional nanocrystals for cancer therapy: A potential nanocarrier. In: *Nanomaterials for Drug Delivery and Therapy*, pp. 91–116, William Andrew Publishing, Norwich, NY (2019)
28. Wei, D.; Sun, W.; Qian, W.; Ye, Y.; Ma, X.: The synthesis of chitosan-based silver nanoparticles and their antibacterial activity. *Carbohydr. Res.* 344(17), 2375–2382 (2009)
29. Fayaz, A.M.; Balaji, K.; Girilal, M.; Yadav, R.; Kalaichelvan, P.T.; Venkatesan, R.: Biogenic synthesis of silver nanoparticles and their synergistic effect with antibiotics: A study against gram-positive and gram-negative bacteria. *Nanomed. Nanotechnol. Biol. Med.* 6(1), 103–109 (2010)
30. Tamayo, L.; Zapata, P.; Vejar, N.; Azócar, M.; Gulppi, M.; Zhou, X.; Thompson, G.; Rabagliati, F.; Pérez, M.: Release of silver and copper nanoparticles from polyethylene nanocomposites and their penetration into *Listeria monocytogenes*. *Mater. Sci. Eng., C* 40, 24–31 (2014)
31. Montazeri, A.; Salehzadeh, A.; Zamani, H.: Effect of silver nanoparticles conjugated to thiosemicarbazide on biofilm formation and expression of intercellular adhesion molecule genes, *icaAD*, in *Staphylococcus aureus*. *Folia Microbiol.* 65(1), 153–160 (2020)
32. Mesaros, N.; Glupczynski, Y.; Avrain, L.; Caceres, N.E.; Tulkens, P.M.; Van Bambeke, F.: A combined phenotypic and genotypic method for the detection of Mex efflux pumps in *Pseudomonas aeruginosa*. *J. Antimicrob. Chemother.* 59(3), 378–386 (2007)
33. Yoneda, K.; Chikumi, H.; Murata, T.; Gotoh, N.; Yamamoto, H.; Fujiwara, H.; Nishino, T.; Shimizu, E.: Measurement of *Pseudomonas aeruginosa* multidrug efflux pumps by quantitative real-time polymerase chain reaction. *FEMS Microbiol. Lett.* 243(1), 125–131 (2005)

**How to cite this article:** Hadad, S., Alkinani, T.A., Mahmoudi, A., Dehghan, S., Moaf, N.M., Naeemi, A.S., Salehzadeh, A.: Biological synthesis of Fe<sub>3</sub>O<sub>4</sub>@Ag using *Scenedesmus obliquus* and evaluation of its effect on the expression of *MexA-B* efflux pump genes in ciprofloxacin-resistant *Pseudomonas aeruginosa* strains. *Micro Nano Lett.* 17, 319–326 (2022).  
<https://doi.org/10.1049/mna2.12138>